

## Supplementary Information

### Supplemental Results

#### *CTCF deficiency in $\gamma\delta$ T cells*

LacZ expression experiments in *Lck-Cre Ctcf<sup>ff</sup>* mice initially suggested that the *Ctcf* gene is expressed in  $\gamma\delta$  T cells (not shown). These results are confirmed using GFP-CTCF as a marker (Figure S4B). In contrast to  $\alpha\beta$  T cells, deletion of the *Ctcf* gene has no adverse effect on  $\gamma\delta$  T cell development, since the number of CD3<sup>+</sup>TCR $\gamma\delta$ <sup>+</sup> thymocytes in *Lck-Cre Ctcf<sup>ff</sup>* mice is ~2-fold higher than in wild type littermates (Figure S2A, B). The relative proportion of  $\gamma\delta$  T cells in the spleens of *Lck-Cre Ctcf<sup>ff</sup>* mice is also markedly increased (Figure S2A), due to impaired  $\alpha\beta$  T cell production. In fact, *in vitro* culture of anti-CD3/CD28 antibody-stimulated peripheral T cell fractions from *Lck-Cre Ctcf<sup>ff</sup>* mice results in a selective outgrowth of TCR $\gamma\delta$  T cells (Supplementary Figure S2C). We do not detect CTCF protein in a mixed population of *in vitro* activated TCR $\alpha\beta$  and TCR $\gamma\delta$  T cells from *Lck-Cre Ctcf<sup>ff</sup>* mice (Supplementary Figure S2D, E). We therefore conclude that CTCF is essential for TCR-mediated activation and proliferative expansion of TCR $\alpha\beta$  but not of TCR $\gamma\delta$  T cells.

#### *CTCF deficient thymocytes and the maintenance of methylation*

CTCF has been proposed to be required for the maintenance of methylation at the *Igf2/H19* locus (Schoenherr et al, 2003). Aberrant methylation of this locus, or of other loci, might therefore cause defects in CTCF-negative T cells. As CTCF deletion is highly efficient in T cells from *Lck-Cre Ctcf<sup>ff</sup>* mice and expression of DNMT1, a maintenance methyltransferase with an important role in T cell development (Lee et al, 2001), is not significantly affected by deletion of CTCF in thymocytes (Figures 1C

and 6A), we used these cells to examine DNA methylation in the *Igf2/H19* locus in the absence of CTCF. We find similar methylation of a CTCF-binding site in the *Igf2/H19* imprinted locus in wild type and CTCF-deleted thymocytes (Supplemental Figure S5A). We also examined the methylation status of the ribosomal DNA (rDNA) repeats in *Ctcf* knockout cells, as these repeats have been shown to be heavily methylated (Bird et al, 1981), and CTCF binds to a region of the rDNA repeat upstream of the transcription start site (Van de Nobelen et al, manuscript in preparation). We do not detect differences in rDNA methylation in the thymus (where CTCF is virtually absent) and spleen (where CTCF is not deleted) from *Lck-Cre Ctcf<sup>ff</sup>* mice (Supplemental Figure S5B). We conclude that a deletion of CTCF does not lead to aberrant methylation patterns. The paralogue of CTCF, named CTCF-L or BORIS, can bind the same DNA sequences as CTCF (Loukinov et al, 2002). However, we do not detect *Ctcf-l* mRNA in T cells in the presence or absence of CTCF (data not shown). Thus, CTCF-L neither acts in a dominant-negative fashion in T cells lacking CTCF, nor does it compensate for loss of CTCF.

#### *CTCF deficient thymocytes and nuclear organization*

Given the important role of CTCF in chromatin organization of the rDNA repeat (Van de Nobelen et al, manuscript in preparation) we examined whether lack of CTCF affects nucleolar organization in T cells. We visualized the rDNA repeats in wild type and CTCF-deficient T cells by fluorescent in situ hybridization (FISH) with an rDNA probe (Akhmanova et al, 2000) (Supplemental Figure S6). Based on the FISH signals we counted the number of rDNA dots in CD4<sup>+</sup> and CD8<sup>+</sup> T cells, derived from *Ctcf* knockout (KO) and wild-type (WT) mice (Supplemental Table SI). We found a very small shift towards a lower number of dots in *Ctcf* knockout cells. Combined our data

indicate that in naive resting T cells nuclear and nucleolar organization are not dramatically perturbed. The effects that we observe are therefore mainly established upon T cell activation, explaining the phenotype observed in ISP cells.

## Supplemental Methods

### *In vitro T cell cultures*

For *in vitro* T cell cultures from wild-type or *lck-Cre Ctc<sup>fl/fl</sup>* mice, either total T cell fractions (Fig. S2C) were purified from lymph node/spleen by MACS depletion (using anti-B220, anti-NK1.1, anti-Ter119, anti-CD11b and anti-Gr-1 antibodies), TCR $\alpha\beta$ -enriched T cell fractions (Fig. S2D) were purified by MACS depletion using the same antibody mix supplemented with anti-TCR $\gamma\delta$  antibodies, or CD4<sup>+</sup> T fractions (Fig. 6D) were purified by MACS depletion using the same antibody mix supplemented with anti-CD8 antibodies. Purity of obtained fractions was >98%, but the TCR $\alpha\beta$ -enriched T cell fractions still contained TCR $\gamma\delta$  low T cells (<2% in wild type and ~30% in CTCF-deficient mice). T cells were cultured at a concentration of  $1 \times 10^6$  cells/ml in Iscove's modified Dulbecco's medium (IMDM) (Bio Whittaker, Walkersville, MD) containing 10% heat-inactivated FCS,  $5 \times 10^{-5}$  M  $\beta$ -mercaptoethanol, 100 U/ml penicillin and 100  $\mu$ g/ml streptomycin. Stimulation was with plate-bound anti-CD3 (145-2C11) and anti-CD28 (37.51) mAbs (coated at 10  $\mu$ g/ml each at 4°C overnight for 7 days).

### *Fluorescent in situ hybridization (FISH)*

FACS sorted naïve CD62L<sup>+</sup> CD4<sup>+</sup> T cells from *CD4-Cre Ctc<sup>fl/fl</sup>* mice were briefly cultured (Ribeiro de Almeida et al, manuscript in preparation) and allowed to attach to glass slides for 30 min. Cells were fixed for 10 min with 4% PFA/PBS. Slides were stored in 70% EtOH until further use. For DNA-FISH slides were pre-treated by two PBS wash-steps followed by a permeabilization step (4 min incubation in 0,1% pepsin in 0,01M HCl at 37 °C). Slides were washed once in PBS on ice and fixed again for 5 min in 4% PFA/PBS. Slides were washed twice in PBS and dehydrated. Denaturation

was done for 2 min at 80 °C in denaturing solution (70% formamide; 2xSSC; 10 mM phosphate buffer, pH 7), after which the slides were cooled in 70% EtOH, dehydrated and hybridised as described (Gribnau et al, 2005). The rDNA probe (an 11.8 kb Sall fragment of a murine rDNA cosmid which contains non transcribed rDNA only (Akhmanova et al, 2000) was DIG labelled by nick translation (Roche). We used a Zeiss Axioplan 2 microscope for image acquisition and cell counting. Cells were counted without knowledge of the genotype, statistical significance was tested with the chi-square tool (Excel), with a p-value of 0.005.

## Supplementary Figures.

### *Figure S1. Schematic overview of T cell differentiation in the thymus.*

T cell progenitors that enter the thymus are called double-negative (DN) cells. These cells differentiate as outlined in the figure in a series of stages towards mature thymocytes, which leave the thymus and migrate to the periphery. The DN1-DN4 early T cell stages are characterized by the differential expression of the CD25/CD44 markers. At DN2 a choice is made whether to rearrange the  $\alpha\beta$  or the  $\gamma\delta$  *Tcr* genes. The  $\gamma\delta$  T cell differentiation pathway is not depicted here. In the case of  $\alpha\beta$  T cells, the  $\beta$  *Tcr* gene is rearranged first (the approximate time frame of rearrangement is indicated below the cells). Upon productive recombination (mediated by the RAG proteins, see main text) a functional  $\beta$  receptor is expressed at the cell surface (red rectangle), where it associates with pT $\alpha$  (black rectangle), a “surrogate” TCR $\alpha$  receptor, required for signalling. Cells subsequently start to grow, and they divide rapidly (indicated by circular arrows). At the double-positive (DP) stage cells cease division and start rearranging their *Tcr $\alpha$*  genes (approximate time frame is indicated below the cells). Productive rearrangement results in the expression of the  $\alpha\beta$  TCR (green and red rectangles). Positive and negative selection result in the formation of a pool of competent CD4 and CD8 single-positive (SP) cells. It should be realized that more than 90% of the DP cell population dies during the processes of selection. The approximate number of cell divisions in the different stages are indicated on the bottom of the scheme. The *Lck*-promoter turns on *Cre* expression in DN1-DN2 (indicated by downward arrow). This T cell developmental scheme is based on (Laurent et al, 2004; Lucas et al, 1993).

### *Figure S2. Characterization of TCR $\gamma\delta$ cells in *Lck-Cre Ctc $f^{ff}$* mice.*

A) Flow cytometric analyses of total thymocytes and CD3<sup>+</sup> splenocytes derived from wild type (WT) and *Lck-Cre Ctc<sup>fl/fl</sup>* mice. For the thymus, expression profiles of CD3 and TCR $\gamma\delta$  surface markers are shown as dot plots. Gating is indicated by the horizontal and vertical lines in the graph. The percentages of CD3<sup>+</sup>TCR $\gamma\delta$ <sup>+</sup> cells are shown. For the spleen, data are displayed as histograms and the percentages represent the fractions of CD3<sup>+</sup> cells that are TCR $\gamma\delta$ <sup>+</sup>. Data shown are representative of all animals.

B) Absolute numbers of TCR $\gamma\delta$ <sup>+</sup> T cells in thymus and spleen of wild type (WT) and *Lck-Cre Ctc<sup>fl/fl</sup>* mice. Each symbol represents a measurement in one animal (9 or more tested per group). Horizontal lines indicate averages. TCR $\gamma\delta$ <sup>+</sup> T cells are significantly increased in the thymus of *Lck-Cre Ctc<sup>fl/fl</sup>* mice (p<0.05).

C) Flow cytometric analysis of TCR $\gamma\delta$  expression in T cell cultures from wild type (WT) and *Lck-Cre Ctc<sup>fl/fl</sup>* mice. Lymph node fractions were stimulated by anti-CD3/CD28 and cultured for 7 days. The percentages represent the fractions of TCR $\gamma\delta$ <sup>+</sup> T cells. The proportions of  $\gamma\delta$ <sup>+</sup> T cells in the T-cell enriched cell suspensions before culture was <2% in WT and ~30% in *Lck-Cre Ctc<sup>fl/fl</sup>* mice (see also panel S2A).

D) Flow cytometric analysis of CD4, CD8 and TCR $\gamma\delta$  expression in mixed T cell cultures from wild-type and *Lck-Cre CTCF<sup>fl/fl</sup>* mice. Lymph node cell fractions were enriched for CD4 and CD8 cells and depleted for TCR $\gamma\delta$ <sup>+</sup> T cells, stimulated by anti-CD3/CD28, and cultured for 7 days. The percentages represent the fractions of different T cells.

E) Western blot, showing the absence of CTCF protein in mixed T cell cultures from wild type (WT) and *Lck-Cre CTCF<sup>fl/fl</sup>* mice. Fibrillarin was used as a loading control. Molecular weight markers are indicated in kDa.

*Figure S3. Comparison of CD3 expression and cell size in wild type and CTCF-deficient thymocytes.*

Quantification of CD3 levels (CD3, A) and forward scatter values (FSC, B) in thymocyte subpopulations of wild type (white bars), heterozygous *Lck-Cre Ctcf<sup>+/-</sup>* (grey bars) and homozygous *Lck-Cre Ctcf<sup>-/-</sup>* (black bars) mice. FSC is a measure of cell size. Plotted are average values  $\pm$  SD from 5 wild type, 4 heterozygous and 3 homozygous mice. Statistically significant differences (t-test) are indicated (p<0.005: \*, p<0.01: \*\*, p<0.001: \*\*\*, p<0.0001: \*\*\*\*). DN: double-negative, ISP: immature single-positive, DP: double-positive, CD4: CD4 single-positive, CD8: CD8 single positive (see also Figure S1).

*Figure S4. Flow cytometric analysis of GFP-CTCF protein expression.*

GFP-CTCF protein was analyzed, in conjunction with cell surface markers, in cell suspensions from thymus (A) and spleen (B) from mice carrying a *GFP-Ctcf* knock-in allele (*Ctcf<sup>GFP</sup>*, H.H. *et al.*, manuscript in preparation, for targeting strategy see (Akhmanova et al, 2005)). The indicated cell populations were gated and expression data are displayed as histogram overlays of GFP-CTCF (green) on top of background signals in wild type mice (black). Note that CTCF is also expressed in  $\gamma\delta$ T cells.

*Figure S5. DNA methylation and CTCFL expression in T cells.*

A) DNA methylation analysis in the Imprinting Control Region (ICR) of the *Igf2/H19* locus. DNA was isolated from the thymus of *Ctcf<sup>-/-</sup>* mice, which were either not crossed (-, lanes 2, 3 and 5) or crossed (+, lanes 4 and 6) with *Lck-Cre* transgenics. Samples were digested with *SacI* only (lane 2) or with both *SacI* and *ClaI* (other



lanes). *Cla*I cuts within CTCF binding site 1 of the *Igf2/H19* ICR (Schoenherr et al, 2003). Normal tail DNA (lane 1) is shown as control.

B) Methylation status of ribosomal DNA (rDNA) repeats. Southern blot analysis of genomic DNA from thymus and spleen of the indicated mice. DNA was digested with *Eco*RI (lanes 1), *Eco*RI and *Hpa*II (lanes 2), or (3) *Eco*RI and *Msp*I (lanes 3). Blots were hybridized with the unstable 5' external transcribed spacer probe (Akhmanova et al, 2000).

*Figure S6. CTCF deletion does not affect nucleolar organization in resting T cells.*

FISH analysis of nucleolar organization in FACS-sorted naive CD62L<sup>+</sup> peripheral T cells from the indicated mice. Slides were hybridized with a DIG-labeled rDNA probe (green) containing non transcribed rDNA (Akhmanova et al, 2000). Cells were counterstained with DAPI (blue).

### Supplementary Tables.

Table SI. Number of nucleoli in wild-type and CTCF-negative T cells.

CD4+	number of rDNA dots (%)								
	0	1	2	3	4	5	6	7	Total
WT	0	2	17	20	32	22	5	1	100 (n=358)
KO	0	3	16	29	26	18	6	1	100 (n=368)

CD8+	number of rDNA dots (%)								
	0	1	2	3	4	5	6	7	Total
WT	1	5	9	27	26	21	7	3	100 (n=351)
KO	0	6	12	27	28	18	8	1	100 (n=354)

## Supplemental References

Akhmanova A, Mausset-Bonnefont AL, van Cappellen W, Keijzer N, Hoogenraad CC, Stepanova T, Drabek K, van der Wees J, Mommaas M, Onderwater J, van der Meulen H, Tanenbaum ME, Medema RH, Hoogerbrugge J, Vreeburg J, Uringa EJ, Grootegoed JA, Grosveld F, Galjart N (2005) The microtubule plus-end-tracking protein CLIP-170 associates with the spermatid manchette and is essential for spermatogenesis. *Genes Dev* 19: 2501-2515

Akhmanova A, Verkerk T, Langeveld A, Grosveld F, Galjart N (2000) Characterisation of transcriptionally active and inactive chromatin domains in neurons. *J Cell Sci* 113: 4463-4474

Bird AP, Taggart MH, Gehring CA (1981) Methylated and unmethylated ribosomal RNA genes in the mouse. *J Mol Biol* 152: 1-17

Gribnau J, Luikenhuis S, Hochedlinger K, Monkhorst K, Jaenisch R (2005) X chromosome choice occurs independently of asynchronous replication timing. *J Cell Biol* 168: 365-373

Laurent J, Bosco N, Marche PN, Ceredig R (2004) New insights into the proliferation and differentiation of early mouse thymocytes. *International immunology* 16: 1069-1080

Lee PP, Fitzpatrick DR, Beard C, Jessup HK, Lehar S, Makar KW, Perez-Melgosa M, Sweetser MT, Schlissel MS, Nguyen S, Cherry SR, Tsai JH, Tucker SM, Weaver WM, Kelso A, Jaenisch R, Wilson CB (2001) A critical role for Dnmt1 and DNA methylation in T cell development, function, and survival. *Immunity* 15: 763-774

Loukinov DI, Pugacheva E, Vatolin S, Pack SD, Moon H, Chernukhin I, Mannan P, Larsson E, Kanduri C, Vostrov AA, Cui H, Niemitz EL, Rasko JE, Docquier FM, Kistler M, Breen JJ, Zhuang Z, Quitschke WW, Renkawitz R, Klenova EM, Feinberg AP, Ohlsson R, Morse HC, 3rd, Lobanenko VV (2002) BORIS, a novel male germline-specific protein associated with epigenetic reprogramming events, shares the same 11-zinc-finger domain with CTCF, the insulator protein involved in reading imprinting marks in the soma. *Proc Natl Acad Sci U S A* 99: 6806-6811

Lucas B, Vasseur F, Penit C (1993) Normal sequence of phenotypic transitions in one cohort of 5-bromo-2'-deoxyuridine-pulse-labeled thymocytes. Correlation with T cell receptor expression. *J Immunol* 151: 4574-4582

Schoenherr CJ, Levorse JM, Tilghman SM (2003) CTCF maintains differential methylation at the Igf2/H19 locus. *Nat Genet* 33: 66-69

Figure S1 - Heath et al - revised

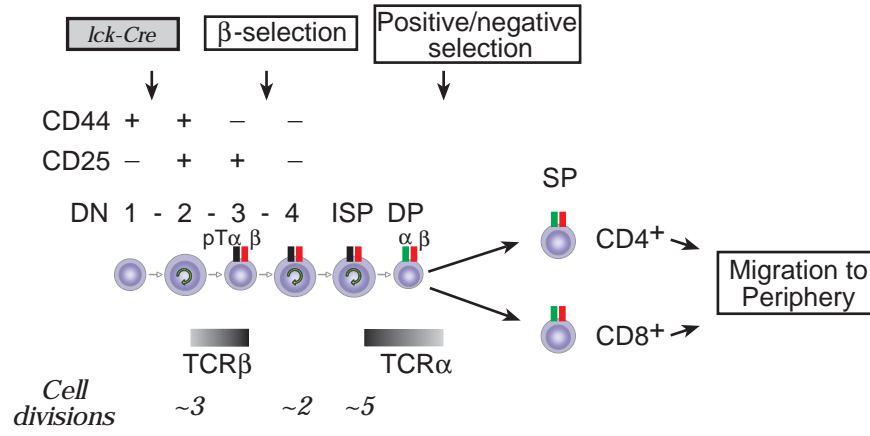


Figure S2 - Heath et al - revised

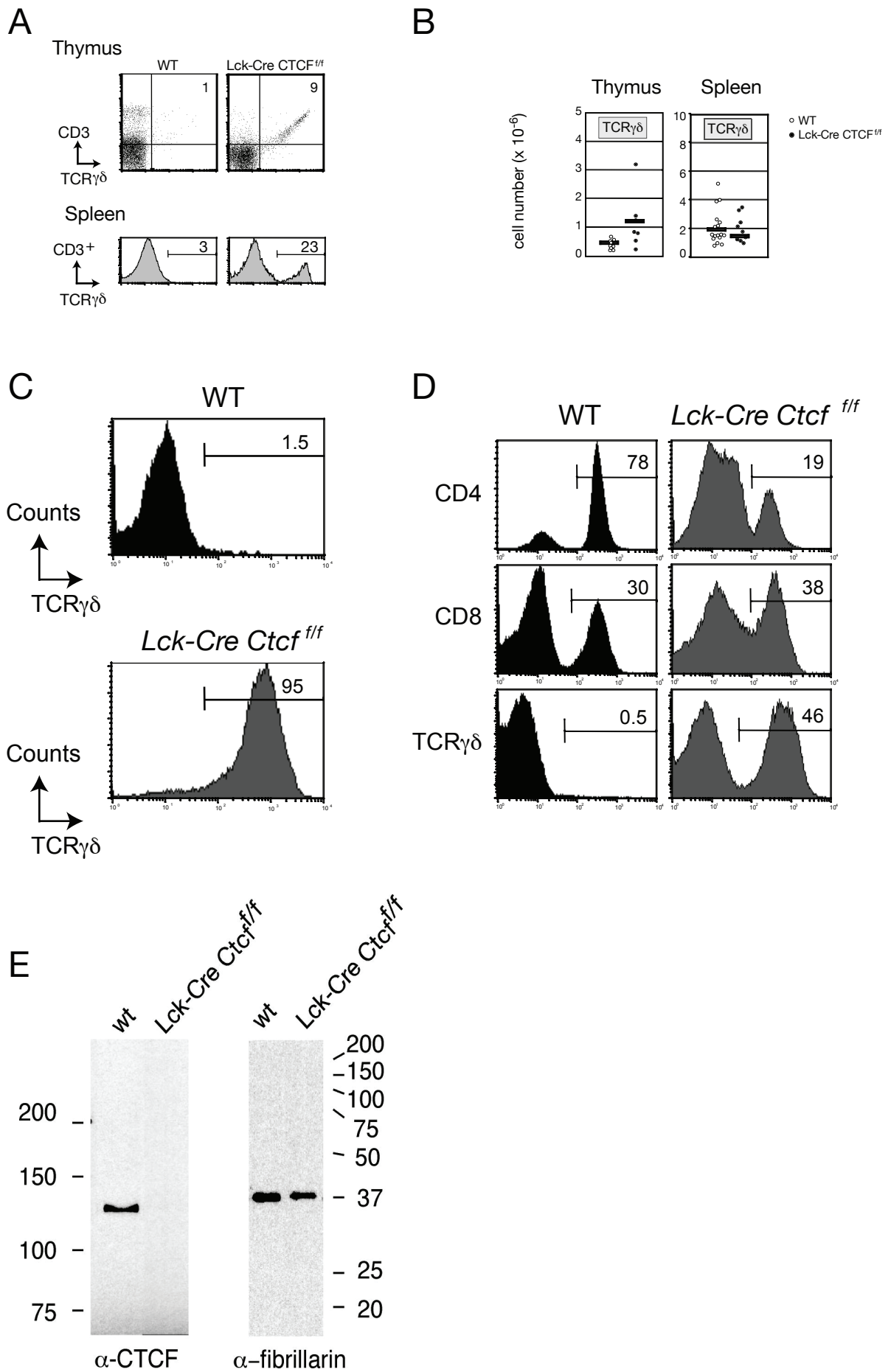
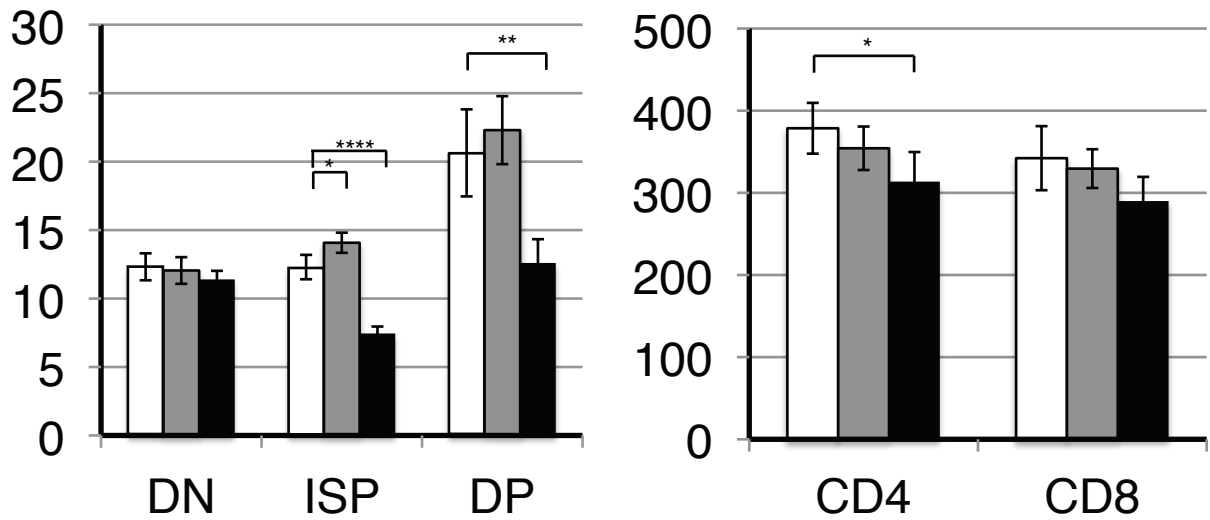


Figure S3 - Heath et al - revised

A

CD3



B

FSC

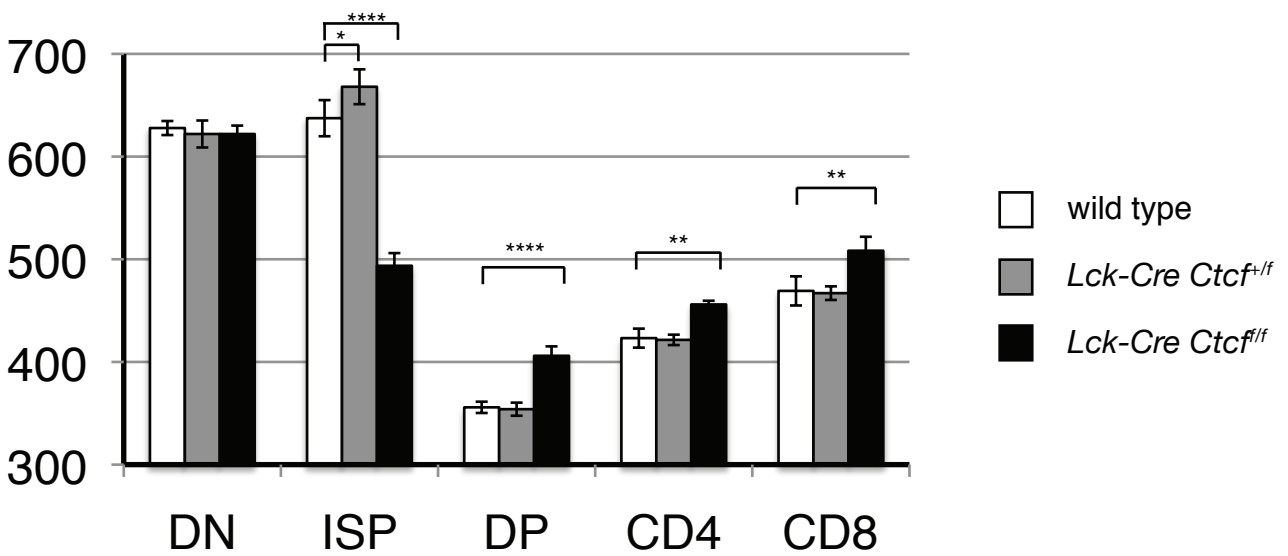


Figure S4 - Heath et al - revised

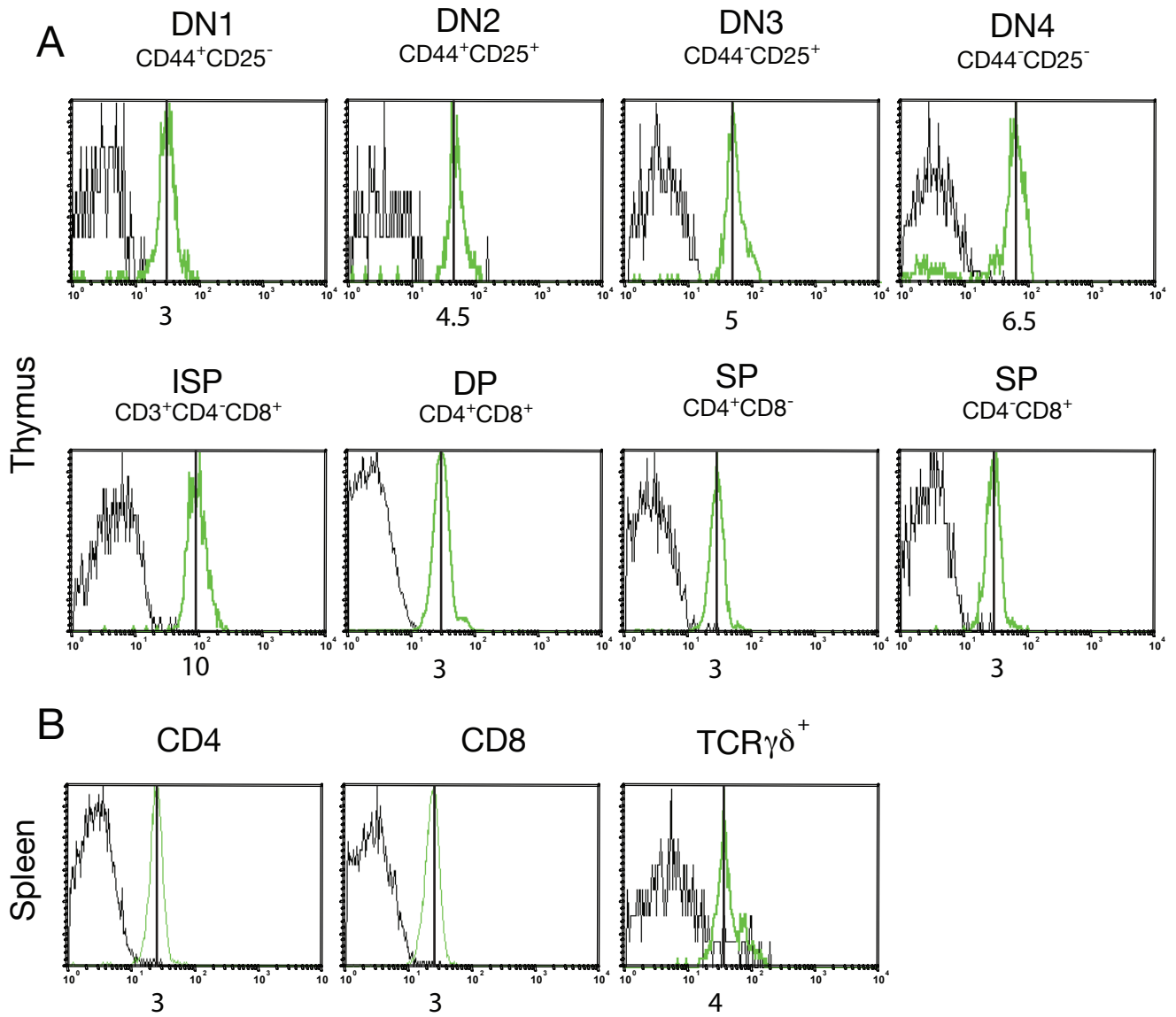


Figure S5- Heath et al - revised

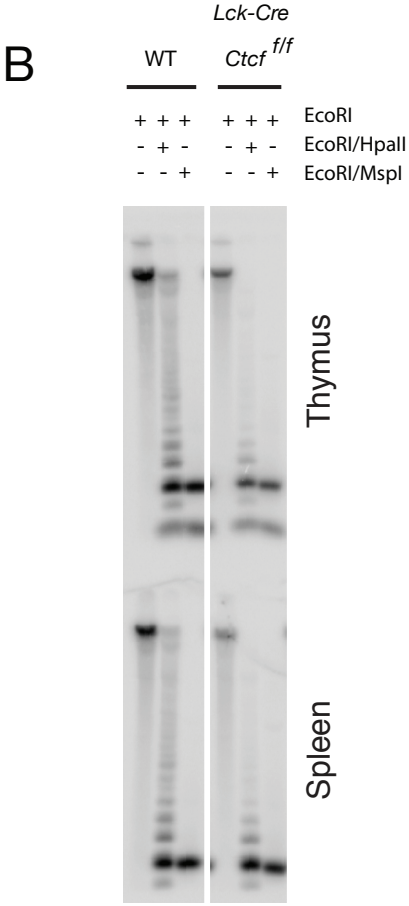
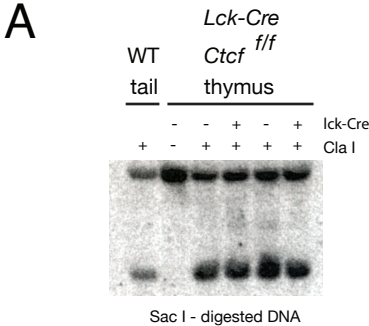




Figure S6 - Heath et al -revised

